



Contents lists available at ScienceDirect

Journal of King Saud University – Science

journal homepage: [www.sciencedirect.com](http://www.sciencedirect.com)

Original article

# Green synthesis and antimicrobial efficacy of titanium dioxide nanoparticles using *Luffa acutangula* leaf extract

Devipriya Anbumani<sup>a</sup>, Kayal vizhi Dhandapani<sup>a</sup>, Janani Manoharan<sup>b</sup>, Ranganathan Babujanarthanam<sup>a,\*</sup>, A.K.H. Bashir<sup>c</sup>, Karnan Muthusamy<sup>d</sup>, Ahmed Alfarhan<sup>e</sup>, K. Kanimozhi<sup>f</sup><sup>a</sup> Nano and Energy Biosciences Laboratory, Department of Biotechnology, Thiruvalluvar University, Serkkadu-632115, Vellore, Tamil Nadu, India<sup>b</sup> Department of Biochemistry, Auxilium College (Autonomous), Gandhi Nagar, Vellore 632006, Tamil Nadu, India<sup>c</sup> Department of Physics, Sudan University of Science and Technology, 11113 Khartoum, Sudan<sup>d</sup> Grassland and Forages Division, National Institute of Animal Science, Rural Development Administration, Cheonan 31000, Republic of Korea<sup>e</sup> Department of Botany and Microbiology, College of Science, King Saud University, P.O. Box 2455, Riyadh 11451, Saudi Arabia<sup>f</sup> Department of Chemistry, Global Institute of Engineering and Technology, Melvisharam 632509, Tamil Nadu, India

## ARTICLE INFO

### Article history:

Received 6 December 2021

Revised 28 January 2022

Accepted 4 February 2022

Available online 9 February 2022

### Keywords:

TiO<sub>2</sub> nanoparticles*Luffa acutangula*

Morphological characterize

Antimicrobial action

Microscopy analysis

## ABSTRACT

The present study deals with the synthesis of titanium dioxide (TiO<sub>2</sub>) nanoparticles using *Luffa acutangula* leaf extract and explore the antimicrobial potential of synthesized nanoparticles. The biosynthesized TiO<sub>2</sub> nanoparticles were characterized using different spectroscopic and microscopic techniques. The absorption spectrum of synthesized TiO<sub>2</sub> nanoparticles were primarily characterized by Ultraviolet visible (UV-vis) spectrophotometer. The functional groups associated with the TiO<sub>2</sub> nanoparticles and the *Luffa acutangula* leaf extract were examined by Fourier Transform Infrared (FTIR) spectroscopy. The crystalline structure of nanoparticles were analyzed by X-ray diffraction (XRD) examination. Morphological characters were examined by Scanning Electron Microscopy (SEM) and Transmission Electron Microscope - Selective Area Electron Diffraction (TEM - SAED). Presence of elemental composition of synthesized TiO<sub>2</sub> nanoparticles were characterized by Energy Dispersive X-ray (EDX). The antimicrobial properties of the TiO<sub>2</sub> nanoparticles were observed to be highly toxic against bacterial strains are *Bacillus subtilis* (*B. subtilis*), *Escherichia coli* (*E. coli*), *Enterococcus faecalis* (*E. faecalis*), *Klebsiella pneumonia* (*K. pneumoniae*), *Staphylococcus aureus* (*S. aureus*) and *Pseudomonas aeruginosa* (*P. aeruginosa*) and the fungal strains are *Aspergillus flavus* (*A. flavus*), *Aspergillus niger* (*A. niger*), *Rhizopus oryzae* (*R. oryzae*) and *Sclerotium rolfsii* (*S. Rolfsii*). The zone of inhibition was estimated by disc diffusion assay and moreover, minimum inhibitory concentration was evaluated by the micro broth dilution assay. It can be concluded that titanium dioxide nanoparticles manifest a strong antimicrobial action and thus can be developed as a novel type of antimicrobial materials for the cure of microbial infections.

© 2022 The Author(s). Published by Elsevier B.V. on behalf of King Saud University. This is an open access article under the CC BY-NC-ND license (<http://creativecommons.org/licenses/by-nc-nd/4.0/>).

## 1. Introduction

Nanotechnology has attained vast attention over time, and it involves synthesizing and developing different nanomaterial (Kasinathan et al., 2016; Panimalar et al., 2022; Rathnakumar et al., 2019; Magdalane et al., 2018; Aina et al., 2018) and it is an

accelerating field of recent research with desirable applications in medicine and electronic and has been developing very fast in recent generation, impacting on distinct areas such as environment and economy (Mani et al., 2021; Magdalane et al., 2021; Loo et al., 2018; Srinivasan et al., 2020). It is fundamentally concerned about the synthesis of nanoparticles (NPs) and their application in different fields of science, medicine, designing and imaging (Ocsoy et al., 2013; Jayakumar et al., 2022). Nanoparticles are characterized as building blocks of nanotechnology and the size ranging from 1 to 100 nm in diameter (Hoffmann et al., 1995; Fabrega et al., 2010; Fang et al., 2012). The foremost feature of nanoparticles is their surface area to volume aspect ratio, enabling them to combine with other particles easier. Moreover, metal nanoparticles have been intensively used in biology because they are biocompatible

\* Corresponding author.

E-mail address: [babukmg@gmail.com](mailto:babukmg@gmail.com) (R. Babujanarthanam).

Peer review under responsibility of King Saud University.



Production and hosting by Elsevier

<https://doi.org/10.1016/j.jksus.2022.101896>

1018-3647/© 2022 The Author(s). Published by Elsevier B.V. on behalf of King Saud University.

This is an open access article under the CC BY-NC-ND license (<http://creativecommons.org/licenses/by-nc-nd/4.0/>).

in nature and can interact with proteins, receptors, and nucleic acids because of their size range (Gelis et al., 2003; Trouiller et al., 2009; Jayaseelan et al., 2013). These nanoparticles are regarded as susceptible to bind targeting agents after appropriate functionalization for delivery of those biomolecules to the targeting sites (Ahmad et al., 2015; Zdyb and Krawczyk, 2014; Dadkhah et al., 2014). Currently, nanoscale particles have been tremendously applied to the advancement of novel antimicrobial agents for the treatment of pathogenic microorganisms. Among the prevailing antimicrobial substances, nanoscale materials are of immense attention because of their eminent effectiveness and reactivity (Gerhardt et al., 2007; Prakash et al., 2012; Chen et al., 2014). Administration of nanoparticles as antibacterial drug is a new and ingenious approach, which is a cost-effective measure against pathogenic microorganisms (Xiaoming, 2015; Pu et al., 2013; Zhao et al., 2015). Over the last few years, titanium dioxide nanoparticles (TiO<sub>2</sub> NPs) have been broadly utilized as an eco-friendly and clean photocatalyst, due to its optical properties, apex chemical stability and less toxic nature (Ahmed et al., 2016; Ahmad et al., 2010; Manjula et al., 2018; George et al., 2022). Moreover, titanium dioxide are the most important materials for beauty care products, drugs, skin care materials specially to protect skin from UV rays, whiteness, opacity to products like paints, food colorants, papers, toothpastes, plastics, and inks (Kaviya et al., 2021; Orudzhev et al., 2020; Mani et al., 2021; Geethalakshmi and Sarada, 2010; Willner et al., 2007). It is likewise utilized in wide potential applications in acaricidal action, antibacterial, pharmaceuticals and solar cell (Ambika and Sundrarajan, 2016; Duan et al., 2015; Weir et al., 2012; French et al., 2009). The less hazardous and biocompatible nature of TiO<sub>2</sub> NPs find its applications in biomedical sciences, for example pharmaceutical industries as well as in bone tissue engineering (Roopan et al., 2012; Velayutham et al., 2012; Kayalvizhi et al., 2022). There are a few strategies available for synthesis of titanium dioxide nanoparticles like chemical micro emulsion, wet chemical method, vapor phase process, hydrothermal process, microwave-assisted technique and solvothermal technique (Kirthi et al., 2011; Singh and Lillard, 2009; Li et al., 2014; Hu et al., 2010; Brown et al., 2012).

Now a days, some consideration has been focused on the biological route for the synthesis of nanoparticles (Nithiyavathi et al., 2021; Orudzhev et al., 2021; Rajeswari et al., 2021). The utilization of environmentally friendly plant materials such as leaves roots and fruits for the synthesis of nanoparticles serves various advantages because of their non-harmful nature as well as safety and ecological properties (Gong et al., 2007; Allahverdiyev et al., 2011; Anitha and Miruthula, 2014; Dandge et al., 2010). The biological technique utilizing plant extracts has received more consideration than physical and chemical strategies. Furthermore, synthetic drugs formulated by employing distinct strategies in the laboratory and these are the medicines which are not existing in nature. Despite the fact that, herbal medicines are less potent in comparison to synthetic drugs in some cases but still these are consider less toxic or having few side effect in contrast to synthetic drugs (Vanajothi et al., 2012; Abdelhalim et al., 2012; James and Cohen, 1980; Rajakumar et al., 2012). Overcome of these limitations, biosynthesized nanoparticles are widely used in the biomedical applications due to its drug compatibility and ecofriendly nature because of harmful synthetic compounds are not used in this technique. Using plant extracts as an emerging technology for synthesis of different metal oxide nanoparticles (Hunagund et al., 2016; Colthup, 1950) because the plant extract containing various phytochemicals for example, flavonoids, tannins, and proteins and so forth, are the main point of interest to control the shape and size of the nanoparticles (Wiley, 2001; Vizhi et al., 2016). Accordingly, the existence of different surfactants and stabilizers are beneficial to have a control over the development of the

nanoparticles. TiO<sub>2</sub> NPs are well recognized as a versatile multifunctional material because of their superior chemical stability under physiological environment (Philip, 2010; Rajakumar et al., 2011). Recent studies reported that the TiO<sub>2</sub> NPs were synthesized from peel extract of *Annona squamosa*, aqueous leaf extract of *Catharanthus roseus* and the microorganism *Bacillus subtilis* for biomedical applications (Jayaseelan et al., 2013; Fu et al., 2001; Salunkhe et al., 2011; Sathishkumar et al., 2009). The high degree of microbial diseases and their multidrug resistant properties make the scientists to develop a new type of antimicrobial agents (Sundrarajan et al., 2017; Gelover et al., 2006). An advanced and emerging approach to drug development is the utilization of metal nanoparticles as new forms of antimicrobial agents. Therefore, the current interest in the researchers due to the developing microbial resistance against metal particles, antibiotics and the development of resistant strains and the TiO<sub>2</sub> NPs have exhibited significant antibacterial action (Zhang and Chen, 2009; Vazquez-Munoz et al., 2014; Holt and Bard, 2005; Vinayagam et al., 2021). Titanium dioxide plays a more supportive role in our environmental purification because of its antifogging effect, photo induced superhydrophilicity and less toxic nature (Singh et al., 2021; Vijayakumar et al., 2020; Geetha et al., 2018). These properties have been applied in eliminating microbes and toxic organic materials from air and water, also in self-sterilizing surfaces in medical centres.

*Luffa acutangula* belongs to the family Cucurbitaceae, is usually known as ridge gourd and it is utilized as vegetable in Asian nations. The whole plant of *Luffa acutangula* L. (*L. acutangula*) is therapeutically significant and is utilized widely in Indian traditional system of medicines (Parasuraman et al., 2019; Anju et al., 2019). For the purpose of killing the parasite, ridged gourd's leaf extract is applied on sores that have occurred due to guinea worms. Also, leaf sap is useful in curing conjunctivitis as an eye-wash. For the preparation of herbal products, the fruits and seeds are extensively used for treating venereal disease, specifically gonorrhoea. It is also noted in Mauritius that these seed are consumed to remove intestinal worms. Besides, the application of leaf juice on skin to cure eczema. The seed as well as the plant is insecticidal, indicating the potential antioxidant activity (Ramesh et al., 2021; Ramesh et al., 2022; Ramesh et al., 2021; Radhakrishnan et al., 2020). The juice of leaves is likewise utilized for jaundice, antitumor, antidiabetic, eczema, and dysentery conditions (Paramanatham et al., 2018; Akhtar et al., 2016; Habimana et al., 2011). Seed oil used for dermatitis, a fruit extract of *L. acutangula* was noted to possess stronger antibacterial and antifungal activity. The scope of this work was to scrutinize the antimicrobial activity of synthesized TiO<sub>2</sub> NPs using leaf extract of *L. acutangula* against pathogens. The current work aims to utilize the biological route for the synthesis of TiO<sub>2</sub> NPs and characterized using various spectroscopic and microscopic methods for the analysis of structure, morphology, and optical properties (Rajkumari et al., 2019; Parasuraman et al., 2019; Renuka et al., 2020; Nalini et al., 2019). The TiO<sub>2</sub> NPs was synthesised by biological reduction which anticipate appropriate capping agent for the stability of the synthesized nanoparticles and exhibits excellent antibacterial and antifungal activities (Buszewski et al., 2018; Lonnen et al., 2005; Mani et al., 2021; Akiba et al., 2005).

## 2. Experimental section

### 2.1. Preparation of leaves extraction

The leaves of *Luffa acutangula* (Family: Cucurbitaceae) were gathered from Nattamangalam Village, Vellore, India, and the gathered plant leaves were approved (PARC/2017/3522) by Professor. P.

Jayaraman, Director, Institute of Herbal Botany, Plant Anatomy and Research centre, Chennai, Tamil Nadu, India. The newly gathered leaves sample was surface cleaned with running faucet water for eliminate soil followed by refined water and shade dried for 7–8 days at room temperature. The dried sample was powdered in a blender and sieved to get uniform size range and put away at 4 °C for additional investigations. From that, 5 g of leaves sample was risen in 100 ml of refined water taken in 500 ml Erlenmeyer flask at 60 °C for 15 min. At that point, the concentrate was separated utilizing Whatman No.1 filter paper. The filtrate was utilized for the synthesis of titanium dioxide nanoparticles.

## 2.2. Biogenic synthesis of titanium dioxide nanoparticles

In the present studies, the synthesis of nanoparticles of titanium dioxide was done using an organic strategy. For biogenic synthesis of titanium dioxide (TiO<sub>2</sub>) nanoparticles, 100 ml of 1 mM titanium sulfate (bought from Hi Media Laboratories Ltd., India) solution was mixed for 2 hrs. From that, 80 ml of titanium sulfate solution was added to 20 ml of aqueous leaves extract at room temperature under blended condition for 6 hrs. After the response of plant extracts with titanium sulfate, the incorporated nanoparticles turned dark green to light green in shading. Moreover, the concoction was exposed to centrifugation at 10,000 rpm for 10 min. Consequently, made pellets were gathered and decontaminated by repeated centrifugation to eliminate unbound phytochemicals and the subsequent pellet was air dried for assessment of TiO<sub>2</sub> NPs.

## 2.3. Characterization of synthesized titanium dioxide nanoparticles

After synthesis, the titanium dioxide nanoparticles were exposed to characterization by different insightful estimations. UV-Visible (UV-Vis) spectroscopy is a methodology employed for assessing the light that is acclimatized and dispersed by a model. The integrated TiO<sub>2</sub> nanoparticles solution was put between a light source and a photograph finder and the intensity of absorbed light is estimated by Shimadzu 3600 spectrometer and worked at a resolution of 1 nm ranging from 200 and 800 nm ranges. The absorbance can be used to measure the concentration of solution by using Beer Lambert's Law. It is the most widely used method to confirm the formation of nanoparticles and to characterize the electronic structure and the optical features of nanoparticles, as the absorption bands are associated to the diameter and aspect ratio of metal nanoparticles. The presence of functional groups and the binding property of the titanium oxide nanoparticles were determined by Fourier Transform Infrared (FTIR) spectroscopy. Infrared spectroscopy was done in JASCO-4600 spectrometer with straightforward wafers containing the titanium dioxide nanoparticles to be dissected and KBr as cover (9:1 dilution). Spectra were recorded at a goal of 4 cm<sup>-1</sup> more than 4000–500 cm<sup>-1</sup>. The structure of the crystalline pertaining to the integrated TiO<sub>2</sub> NPs were gotten by utilizing X-ray diffraction (XRD) (Bruker D8, Advance) spectroscopy which utilized Cu K $\alpha$  ( $\lambda = 1.5406 \text{ \AA}$ ) radiation for the Bragg's Law ranging from 10 to 80° on the 2 $\theta$  scale and working at 40 kV and at a current of 30 mA. The phase of the nanocrystalline particles were likewise confirmed by utilizing XRD. The morphological characters of the synthesized TiO<sub>2</sub> NPs were analyzed by utilizing scanning electron microscopy (ZEISS (EBO 180) Scanning Electron Microscopy (SEM) equipped with EDX) and elemental components of the synthesized nanoparticles were recognized by Energy Dispersive X-ray (EDX) investigation with a same Model. The TiO<sub>2</sub> NPs were dried and to acquire a powdered structure. At that point, 10 mg of the TiO<sub>2</sub> NPs were redispersed in ethanol and were placed in thin films on carbon coated copper grids. SEM micrographs were obtained with a finder of helper electrons at magnification of 50,000 $\times$ , where the

accelerating voltage was 5 kV and the working distance was adjusted to around 3 mM. The shape, size and distribution of the synthesized TiO<sub>2</sub> NPs were explored by transmission electron microscopy (TEM) (TEM, FEI Tecnai 20 G2 20 S-TWIN High Resolution Transmission Electron Microscopy). A drop of diluted aqueous solution consisting of synthesized TiO<sub>2</sub> NPs were set on the Holey carbon TEM grid followed by drying prior to placing them into the TEM test chamber. TEM microscopic pictures were taken by analyzing the prepared grids and were recorded at an acceleration voltage of 200 kV. Chosen zone of electron diffraction was a crystallographic experimental technique accomplished inside a TEM. Selective Area Electron Diffraction (SAED) was utilized to distinguish crystal structures and examine crystal defects of nanosized particles.

## 2.4. Antimicrobial activity of synthesized TiO<sub>2</sub> nanoparticles

### 2.4.1. Antibacterial activity by disc diffusion assay

The antibacterial action of the synthesized TiO<sub>2</sub> nanoparticles were evaluated against the bacterial pathogens of *Bacillus subtilis* (*B. subtilis*) (ATCC 6051), *Escherichia coli* (*E. coli*) (MTCC-1677), *Enterococcus faecalis* (*E. faecalis*) (ATCC 2912), *Klebsiella pneumonia* (*K. pneumonia*) (NCTC 9633), *Staphylococcus aureus* (*S. aureus*) (MTCC-3160) and *Pseudomonas aeruginosa* (*P. aeruginosa*) (MTCC-4030) strains. Disc diffusion technique was adopted to monitor the antibacterial activity of synthesized titanium dioxide nanoparticles. Exponential bacterial cultures were seeded into Muller Hinton agar and impregnated with sterile discs. The discs were loaded with titanium dioxide nanoparticles with various concentrations (20, 30 and 40  $\mu\text{g/ml}$ ) and empty sterile disc was used as a control. The impregnated discs were kept on the surface of the agar and incubation of the plates was done overnight at room temperature. The experiment was performed in triplicates and the formation of the clear zone of inhibition was computed.

### 2.4.2. Minimal inhibitory concentration against bacterial pathogens

The lesser concentration of each antibacterial agent that hinder the development of the microorganisms were tested by Minimum Inhibitory Concentration (MIC) using microbroth dilution method and was detected by lack of turbidity matching with a negative control. The TiO<sub>2</sub> nanoparticles were dissolved in 10% Dimethyl sulfoxide (DMSO). The MIC of TiO<sub>2</sub> NPs were determined as the minimal concentration of the TiO<sub>2</sub> NPs repressing the visual development of the test cultures like *S. aureus* (MTCC-3160), *K. Pneumoniae* (NCTC 9633), *P. aeruginosa* (MTCC-4030), *E. faecalis* (ATCC 2912), *B. subtilis* (ATCC 6051), and *E. coli* (MTCC-1677). The titanium dioxide nanoparticles were dissolved in 10% DMSO. The various concentrations of 100, 80, 60, 40, 20, 10 and 5  $\mu\text{g/ml}$  were serially diluted in a 96 well plate and inoculated with 5  $\mu\text{l}$  of bacterial culture. After inoculation, the plates were incubated for 24 hrs at 37 °C for cultural growth. The intensity of the culture of each well was read at 600 nm and it compared with the untreated control.

### 2.4.3. Antifungal action by disc diffusion assay

The potato dextrose agar (PDA) was prepared, sterilized, and poured on to sterile petri plates. The cultures of *Aspergillus flavus* (*A. flavus*) (ATCC 10124), *Aspergillus niger* (*A. niger*) (ATCC 1015), *Rhizopus oryzae* (*R. oryzae*) (ATCC 24563) and *Sclerotium rolfsii* (*S. rolfsii*) (ATCC 62666) were swabbed on the PDA plates. The various concentrations of 20, 30 and 40  $\mu\text{g/ml}$  of titanium dioxide nanoparticles were loaded on sterile disc separately and placed inverted on the swabbed plate. Empty sterile disc was kept as control. The plates were kept for 48 hrs incubation and the zone of inhibition was estimated.

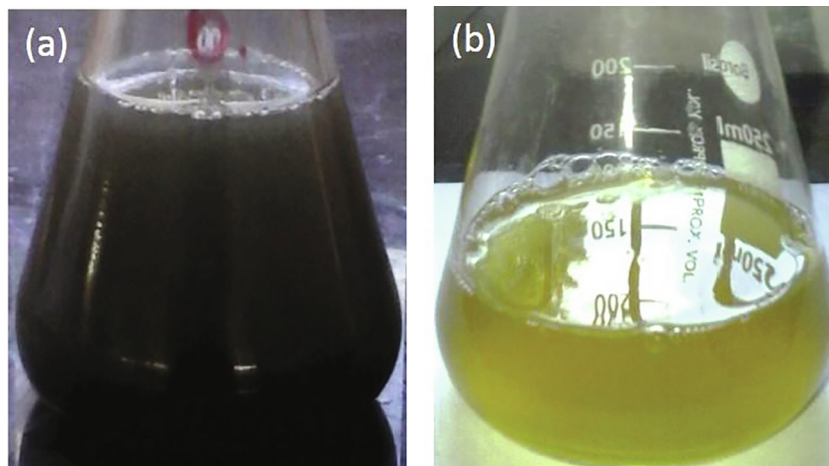


Fig. 1. Visual observation of (a) Titanium sulphate solution with *L. acutangula* leaves extract (b) Biosynthesized titanium dioxide nanoparticles.

### 2.5. Statistical examination

Statistical analysis was done by the SPSS (Statistical Package for Social Sciences) version 20.0, Chicago, IL, USA programming. Examinations were done in sets of three and the information was communicated as mean ± standard error (SE) by the One-Way ANOVA test and the individual correlations were obtained by Duncan’s technique. A difference was deliberated as significant at  $p < 0.05$ .

## 3. Results and discussion

### 3.1. Optical properties of synthesized TiO<sub>2</sub> NPs

UV–visible spectroscopic examination was an efficacious technique to explore if the precursors are totally diminished. The colour change was observed by visible in *L. acutangula* leaves extract during the incubation with titanium sulfate solution. The pure titanium sulfate without aqueous leaves concentrate of *L. acutangula* did not show any colour difference (Fig. 1a) and there was no confirmation for the synthesis of titanium dioxide nanoparticles. Following the reaction of *L. acutangula* extract with titanium sulfate, the colour was changed into light green during 6 hrs stirred conditional incubation period after which there was no noteworthy changes occurred (Fig. 1b) (Hu et al., 2010; Brown et al., 2012). This characteristic colour variation was because of the excitation of the surface plasmon resonance in the synthesis of TiO<sub>2</sub> NPs. Now, the UV–visible absorption of TiO<sub>2</sub> nanoparticles were recorded in an optical range from 200 to 600 nm. Fig. 2 represents the UV–visible absorption spectrum of TiO<sub>2</sub> nanoparticles. The maximum absorption peak was observed at 322 nm, which was a preliminary sign for the synthesis of TiO<sub>2</sub> nanoparticles. In previous research for the green synthesized TiO<sub>2</sub> nanoparticles, noticed that the absorption peak was at 342 nm. As contrasted on previous report, the synthesized titanium dioxide nanoparticles show comparative absorption peak (Nithiyavathi et al., 2021).

### 3.2. Functional groups analysis

FTIR technique was performed to analyse the occurrence of functional groups that was the reasonable for the reduction of TiO<sub>2</sub> nanoparticles. The results were recorded in the range of 4000 to 400 cm<sup>-1</sup> at a resolution of 2 cm<sup>-1</sup> in the KBr pelletization technique. Fig. 3 represents the FTIR spectrum of *L. acutangula* leaves concentrate and TiO<sub>2</sub> NPs. The FTIR range of the synthesized TiO<sub>2</sub> nanoparticles shows the band intensities in various regions

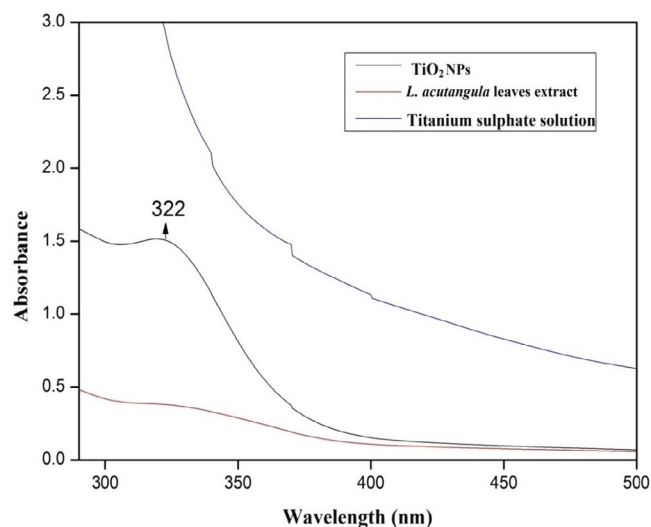


Fig. 2. UV–Vis absorption spectra of the synthesized TiO<sub>2</sub> NPs, *L. acutangula* leaves extract and Titanium sulphate solution.

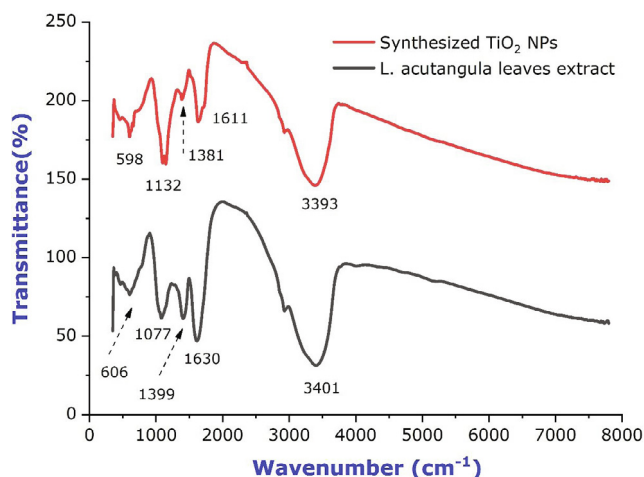


Fig. 3. FTIR spectra of *L. acutangula* leaves extract and synthesized titanium dioxide nanoparticles.

such as 598, 1132, 1381, 1611, and 3393  $\text{cm}^{-1}$  and the peaks were corresponded to the presence of alkyl halides, carboxylic acid, nitro group, amines, and phenol may have taken part during the process of nanoparticle synthesis. The spectral bands were noticeable for *L. acutangula* leaves extract at 606, 1077, 1399, 1630, and 3401  $\text{cm}^{-1}$  and those were corresponded to the presence of alkyl halides, aliphatic amines, alkanes, amide, and amine. The presence of organic groups were because of titanium particle reduction through organic source (Kirthi et al., 2011; Nithiyavathi et al., 2021; Gong et al., 2007). Consequently, it very well might be expected that the compounds were the capping ligands of the nanoparticles (Allahverdiyev et al., 2011; James and Cohen, 1980; Rajakumar et al., 2012). In the current investigation, the association of titanium dioxide nanoparticles with the biomolecules of *L. acutangula* leaves extract indicated that the intense peaks at 598, 1132, 1381, 1611, and 3393  $\text{cm}^{-1}$  relative shift in position and intensity distribution were confirmed by FTIR. The primary difference between the spectra was the proper conversion of varied peaks, this occurrence shows that biomolecules in *L. acutangula* leaves extract such

as alkaloids, phenols, saponins, tannins, terpenoids and triterpenoids were responsible for the biotransformation of  $\text{TiO}_2$  NPs.

### 3.3. Structural analysis

The synthesis of  $\text{TiO}_2$  nanoparticles by *L. acutangula* leaf extract was examined by XRD estimations. The crystal phase composition of  $\text{TiO}_2$  NPs were determined by the XRD estimations was done over the diffraction angle ( $2\theta$ )  $10^\circ$  to  $80^\circ$  utilizing the  $\text{Cu K}\alpha$  radiation. The Bragg's reflections at  $2\theta$  estimations of  $25.47^\circ$ ,  $28.30^\circ$ ,  $29.51^\circ$ ,  $31.65^\circ$ ,  $40.42^\circ$ ,  $48.98^\circ$  and  $54.69^\circ$  could be indexed to the (101), (110), (222), (100), (111), (200) and (105) orientations. These outcomes confirmed the presence of nano-crystalline type of  $\text{TiO}_2$  nanoparticles (Fig. 4). The principle peak of  $2\theta = 28.30^\circ$  matches the (110) crystallographic plane of rutile type of  $\text{TiO}_2$  NPs, representing that the nanoparticles structure was in rutile structure when compared with the Joint Committee on powder Diffraction Standards (JCPDS) data (File No. 89-4202) (33). This pattern reflects the shape of the wave elements of the electronic eigenstates of  $\text{Ti}\backslash\text{O}\backslash\text{Ti}\backslash\text{O}$  chain on the  $\text{TiO}_2$  (110)/ $\text{H}_2\text{O}$  interface (Anitha and Miruthula, 2014; Dandge et al., 2010). The diffraction patterns were consistent with the planes (111) and (110) of pure Face-Centered Cubic (FCC) titanium structure (Vanajothi et al., 2012).

### 3.4. SEM-EDX investigation

Several researchers talked about the shape and size of nanoparticles using scanning electron microscopy (Abdelhalim et al., 2012; James and Cohen, 1980). In the current investigation, the SEM examine was carried out to understand the morphology and size distribution of titanium dioxide nanoparticles. Fig. 5a and b represents the SEM picture of  $\text{TiO}_2$  NPs, the SEM picture indicated that it was made out of NPs mostly aggregates, precise shape and size, which ascribed because of the significant function of *L. acutangula* leaves extract with the help of biological activity. The particles size decreases inversely correlated to increase the surface to volume ratio (Rajakumar et al., 2012; Hunagund et al., 2016). The synthesized  $\text{TiO}_2$  NPs were having a hexagonal cluster and the size range of around 10 to 49 nm, which magnified in 10,000 $\times$ . EDX was utilized to investigate the constituents of elements from the synthe-

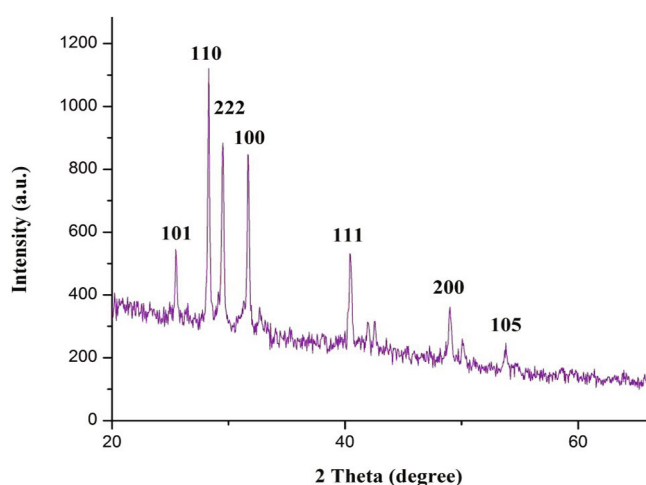


Fig. 4. XRD pattern of the synthesized  $\text{TiO}_2$  NPs.

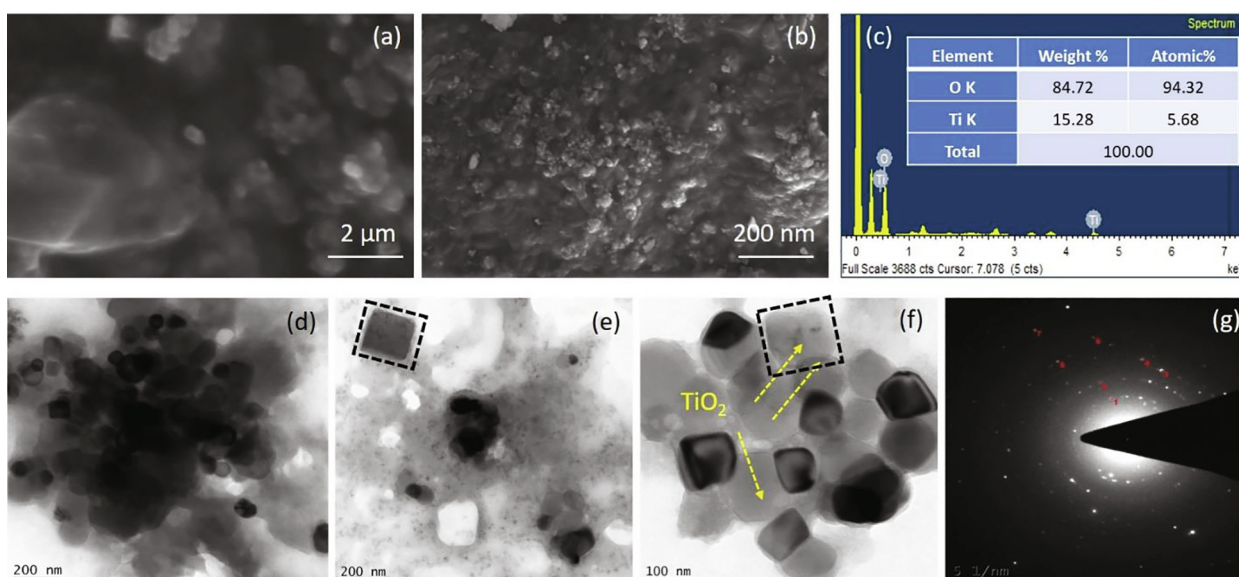


Fig. 5. Characterization analysis (a) and (b) SEM micrograph of synthesized  $\text{TiO}_2$  NPs, (c) Energy-dispersive X-ray spectroscopy exhibiting the chemical components of the synthesized  $\text{TiO}_2$  NPs, (d)–(f) Transmission electron microscopic analysis of  $\text{TiO}_2$  NPs, and (g) SAED pattern of  $\text{TiO}_2$  NPs.

sized TiO<sub>2</sub> NPs. Fig. 5c represents that the EDX spectrum of TiO<sub>2</sub> NPs, the peaks around 0.5 and 0.6 were relevant to the binding energies of titanium and oxygen resembles to the titanium dioxide NPs. The peaks recorded at 7 keV corresponded to the copper grid used for analysis. This outcome confirmed the existence of elemental compounds in the titanium dioxide NPs lacking any impurity peaks and specifies that the synthesized NPs were high purity and the weight and atomic weight percentage (%) was appeared in Fig. 5c.

### 3.5. TEM-SAED examination

TEM is one of the important amazing assets which gives the structure and size information of the nanoparticles. Consequently, the definite shape and size of TiO<sub>2</sub> NPs were done with TEM. The TEM picture of TiO<sub>2</sub> NPs states that the nanoparticles were hexagonal in shape, with a size range of about 10 to 49 nm, in which not many nanoparticles were agglomerated (Fig. 5d-f). At highest magnification, the TEM micrograph exposed that TiO<sub>2</sub> NPs were not in

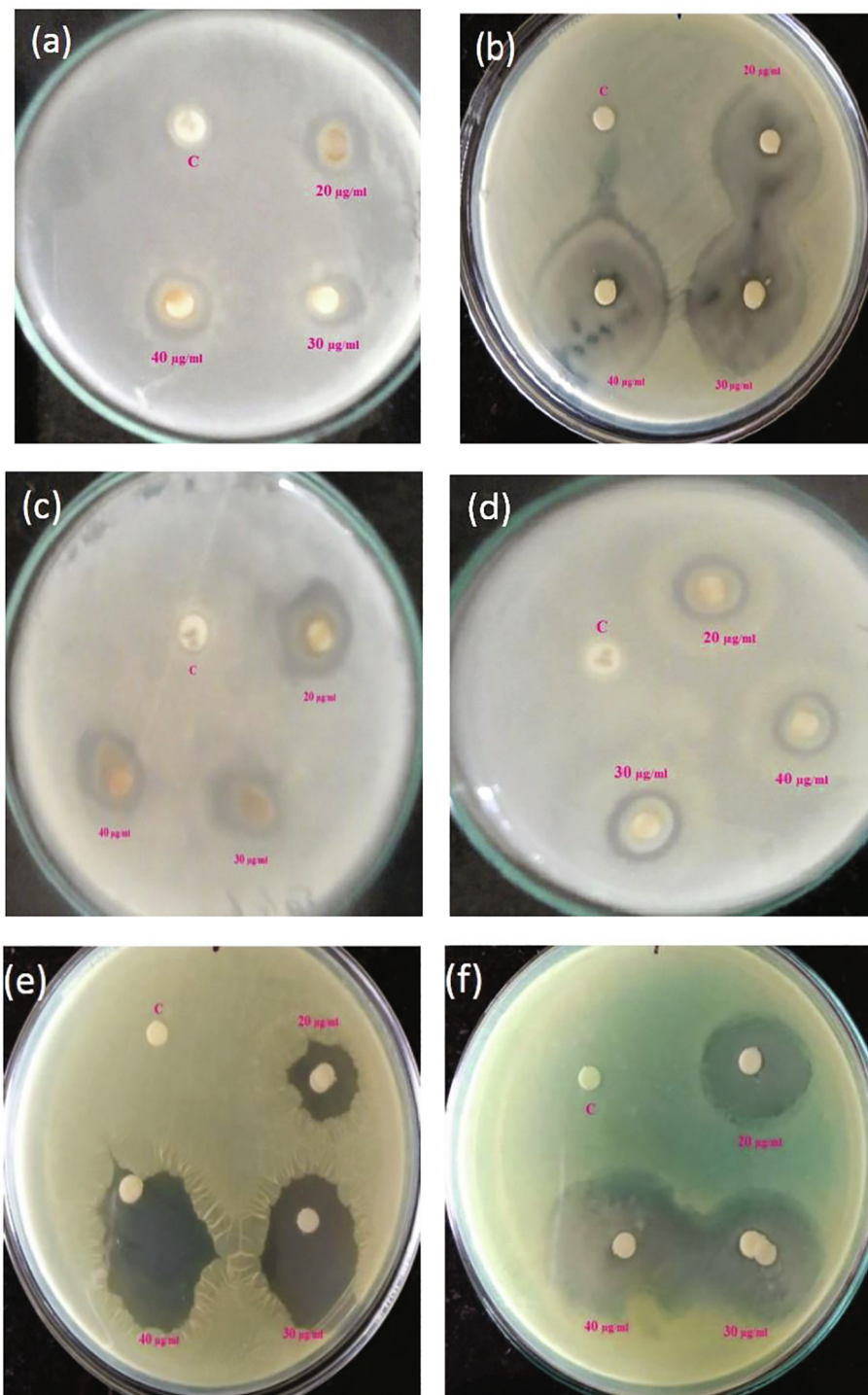


Fig. 6. Zone of inhibition observed against (a) *B. subtilis* (b) *E. coli* (c) *E. faecalis* (d) *K. pneumonia* (e) *S. aureus* and (f) *P. aeruginosa*.

very close physical connection but rather isolated by constant distance with certain divergences. The capping of TiO<sub>2</sub> NPs have likewise been seen under TEM micrograph. This capping might be due to the presence of phytochemicals in the extract. Fig. 5g displays the SAED pattern for the synthesised TiO<sub>2</sub> NPs. The noticed TiO<sub>2</sub> NPs were a constant hexagonal in structure with a diameter ranging from 5 to 7 nm. On the other hand, a diffused rings and a brilliant spot in the SAED pattern specify that the nanoparticles were well crystallized in nature.

### 3.6. Antibacterial activity of titanium dioxide nanoparticles

The antibacterial activity of TiO<sub>2</sub> NPs was evaluated against pathogens by disc diffusion assay such as *B. subtilis*, *E. coli*, *E. faecalis*, *K. pneumoniae*, *S. aureus* and *P. aeruginosa*. The mean of triplicates of obvious zone of inhibition (in millimetres) around each disc was estimated for each of the pathogens (Fig. 6). The capability of the TiO<sub>2</sub> nanoparticles to inhibit bacterial growth has been listed in Table 1. Highest zone of inhibition was observed by the highest concentration of titanium dioxide nanoparticles and the maximum zone of inhibition was observed against *E. coli* (45 ± 0.21), followed by *P. aeruginosa* (43 ± 0.45), *S. aureus* (42 ± 0.13), *K. pneumoniae* (27 ± 0.54), *E. faecalis* (21 ± 0.41) and *B. subtilis* (18 ± 0.56) at 40 µg/ml concentration. Colthup et al., reported that TiO<sub>2</sub> NPs are the mostly examined for their photocatalytic antimicrobial action among different nanoparticles (Colthup, 1950). Wiley et al., have suggested that the potential mechanisms involving the interactions between nanoparticles and biological molecules (Wiley, 2001). The microbes have a negative charge while metal oxide nanoparticles have a positive charge which creates an electromagnetic reaction between the microbes and treated material surface, once the reaction was created, the microbe was oxidized and finally leads to cell death. The interaction of nanoparticles with phosphorus or sulphur containing compounds like DNA and thiol groups of proteins can causes damage of microbe by inhibition of

**Table 1**  
Zone of inhibition observed against different bacterial pathogens with different concentrations by disc diffusion method.

Pathogens	Zone of inhibition (mm)		
	TiO <sub>2</sub> NPs (µg/ml)		
	20	30	40
<i>E. faecalis</i>	13 ± 0.35	18 ± 0.32	21 ± 0.41
<i>B. subtilis</i>	15 ± 0.46	16 ± 0.38	18 ± 0.56
<i>P. aeruginosa</i>	33 ± 0.33	36 ± 0.35	42 ± 0.45
<i>E. coli</i>	35 ± 0.44	42 ± 0.41	45 ± 0.21
<i>S. aureus</i>	21 ± 0.53	33 ± 0.48	42 ± 0.13
<i>K. pneumoniae</i>	19 ± 0.23	21 ± 0.54	27 ± 0.54

Results are expressed as mean ± SE.

**Table 2**  
MIC of TiO<sub>2</sub> NPs against bacterial pathogens with different concentrations.

Pathogens	% of cell inhibition						
	TiO <sub>2</sub> NPs (µg/ml)						
	100	80	60	40	20	10	5
<i>S. aureus</i>	86.75 ± 0.36 <sup>a</sup>	85.30 ± 0.27 <sup>a</sup>	84.33 ± 0.24 <sup>a</sup>	41.66 ± 0.36 <sup>b</sup>	20.56 ± 0.22 <sup>c</sup>	13.37 ± 0.46 <sup>d</sup>	8.54 ± 0.35 <sup>e</sup>
<i>K. pneumoniae</i>	86.70 ± 0.48 <sup>a</sup>	76.09 ± 0.38 <sup>a</sup>	63.91 ± 0.30 <sup>b</sup>	45.00 ± 0.37 <sup>c</sup>	30.13 ± 0.41 <sup>d</sup>	15.56 ± 0.33 <sup>e</sup>	7.23 ± 0.45 <sup>f</sup>
<i>E. coli</i>	83.73 ± 0.49 <sup>a</sup>	73.90 ± 0.57 <sup>b</sup>	64.62 ± 0.18 <sup>c</sup>	53.03 ± 0.25 <sup>d</sup>	33.89 ± 0.37 <sup>e</sup>	18.24 ± 0.36 <sup>f</sup>	3.89 ± 0.26 <sup>g</sup>
<i>B. subtilis</i>	93.06 ± 0.34 <sup>a</sup>	83.57 ± 0.27 <sup>b</sup>	79.82 ± 0.35 <sup>c</sup>	59.74 ± 0.40 <sup>d</sup>	37.39 ± 0.45 <sup>e</sup>	23.34 ± 0.36 <sup>f</sup>	15.56 ± 0.32 <sup>g</sup>
<i>E. faecalis</i>	90.40 ± 0.19 <sup>a</sup>	87.51 ± 0.38 <sup>a</sup>	74.16 ± 0.25 <sup>b</sup>	57.40 ± 0.40 <sup>c</sup>	28.96 ± 0.30 <sup>d</sup>	15.86 ± 0.46 <sup>e</sup>	9.34 ± 0.36 <sup>f</sup>
<i>P. aeruginosa</i>	84.61 ± 0.52 <sup>a</sup>	72.09 ± 0.35 <sup>a</sup>	66.81 ± 0.24 <sup>b</sup>	53.52 ± 0.38 <sup>c</sup>	29.82 ± 0.36 <sup>d</sup>	17.84 ± 0.24 <sup>e</sup>	6.56 ± 0.24 <sup>f</sup>

Result are expressed as mean ± SE (N = 3). p < 0.05 statistically significant difference in groups and different letters shows significant different groups revealed by Duncan's method.

DNA replication and protein inactivation (Vizhi et al., 2016). They are the reason for the pits in bacterial cell walls, which leads to increased cell permeability and cell death (Philip, 2010). The recent reports were suggested that the metal nanoparticles have a durable electrostatic interaction with the cell wall of the bacteria and causes cell death (Rajakumar et al., 2011; Jayaseelan et al., 2013; Fu et al., 2001). Thus, the antibacterial action of TiO<sub>2</sub> NPs possesses excellent ability to be utilized as antibacterial agents against microbes.

### 3.7. Determination of minimal inhibitory concentration

Minimal inhibitory concentration was evaluated by microbroth dilution method using synthesized titanium dioxide nanoparticles suspension against pathogens such as *S. aureus*, *K. pneumoniae*, *P. aeruginosa*, *E. faecalis*, *B. subtilis* and *E. coli* with different concentrations of 100 to 5 µg/ml were tested and the results are given in Table 2. Turbidity within the sample would indicate development of the microorganisms. The lack of turbidity would indicate that the microorganism growth has been inhibited. The outcomes shows that the tested microorganisms were entirely inhibited at 100 to 5 µg/ml concentrations of TiO<sub>2</sub> NPs. The MIC of TiO<sub>2</sub> NPs against *E. coli* was the best affect, followed by *P. aeruginosa* at 5 µg/ml concentration. The moderated effect had been showed by *K. pneumoniae* and *S. aureus* and the lower effect was recorded by *E. faecalis* and *B. subtilis* at 5 µg/ml concentration. The concentration at 5 µg/ml of TiO<sub>2</sub> NPs showed inhibition kinetics against all the tested microorganisms but no significant antibacterial action was observed at concentration less than 5 µg/ml of TiO<sub>2</sub> NPs. The bactericidal effect of titanium dioxide has been attributed to the breakdown of bacterial outer cell membranes by the involvement of reactive oxygen species, hydroxyl radicals, which leads to cell death (Dandge et al., 2010). MIC results obtained in our study resembled those reported by Akhtar and colleagues (Salunkhe et al., 2011). The reported results of MIC are higher than those obtained by us in the present investigation, which suggests that the antimicrobial action of TiO<sub>2</sub> NPs may be influenced by preparation technique as well as by particle size. The difference in MIC results against the test microorganisms might be due to the strains used. Consequently, we can conclude from the results of this investigation that the TiO<sub>2</sub> NPs inhibited the growth and multiplication of all the tested microorganisms.

### 3.8. Antifungal activity of titanium dioxide nanoparticles

The antifungal action of TiO<sub>2</sub> NPs was estimated by measuring the diameter of zone of inhibitions like *A. flavus*, *A. niger*, *R. oryzae* and *S. rolfisii*. Fig. 7 shows that the obvious zone of inhibition (in millimetres) around each disc and it was estimated for each of the strains. Each concentrations showed zone of inhibition against all the fungal pathogens. The maximum zone of inhibition was

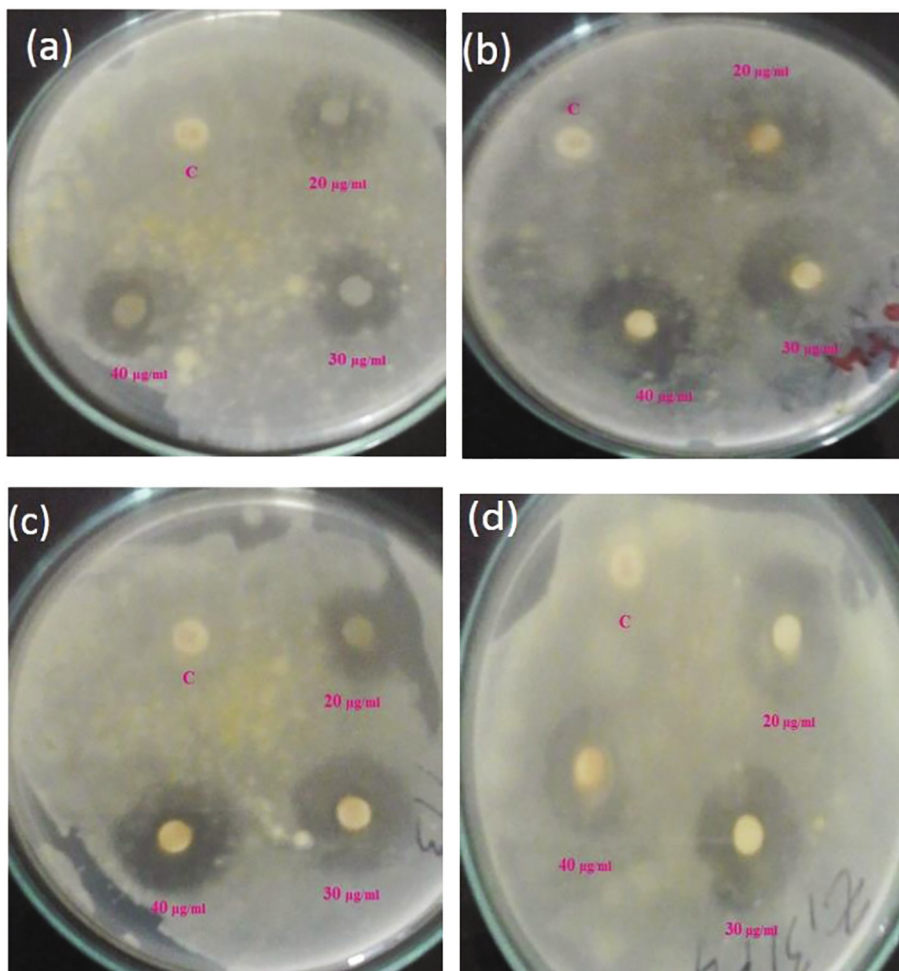


Fig. 7. Zone of inhibition observed against different fungal pathogens (a) *A. niger*, (b) *A. flavus*, (c) *R. oryzae*, and (d) *S. rolfisii*.

shown against *S. rolfisii* ( $42 \pm 0.25$ ), followed by *A. flavus* ( $36 \pm 0.56$ ), *R. oryzae* ( $34 \pm 0.71$ ) and *A. niger* ( $27 \pm 0.36$ ) at  $40 \mu\text{g/ml}$  concentration (Table 3). Highest zone of inhibition was observed by the highest concentration of  $\text{TiO}_2$  nanoparticles. Nowadays antimicrobial action of nanoparticles has been attracted interests to develop a new type of method for controlling infections by preventing at preliminary stage and inhibition of spreading of diseases (Sathishkumar et al., 2009). Because of their differential physical, chemical and biological functions of NPs were utilized in drug products, clinical diagnostic imaging and clinical treatments. The presence of inhibition of zone on culture medium shown the antifungal action of titanium dioxide NPs. To increase the inhibition of fungi growth depends upon the concentration of nanoparticles and furthermore concentration of fungal spores (Sundrarajan et al.,

2017). As indicated by the investigations  $\text{TiO}_2$  NPs have antimicrobial efficiency which could be known as a self-cleaning material (Gelover et al., 2006). The antifungal action of tissue conditioner coating material with titanium dioxide photocatalyst reduce the viable fungal cells under UV light exposure (Zhang and Chen, 2009).

#### 4. Conclusions

The investigation was initiated by the synthesis of  $\text{TiO}_2$  nanoparticles from *L. acutangula* leaves extract by biological route. The biological route was an attractive method for obtaining titanium dioxide nanoparticles with high surface region, porosity and monodispersity. The *L. acutangula* leaves extract was utilized as valuable, reducing agent for the synthesis of  $\text{TiO}_2$  NPs. This biological reduction of  $\text{TiO}_2$  NPs would be a boon for the improvement of clean, harmless and environment friendly  $\text{TiO}_2$  NPs. The synthesised  $\text{TiO}_2$  NPs were exposed to different characterizations such as UV-visible spectroscopy, FTIR investigation, XRD examination, SEM-EDX investigation and TEM-SAED investigation for their optical properties, functional groups, structure, surface morphology and elemental examinations. These outcomes suggest that they were having crystalline structure and hexagonal shape with the size of around 10–59 nm. Antimicrobial action of the synthesized titanium dioxide nanoparticles were determined against test pathogens. Disc diffusion assay and MIC were commonly used to assess the antimicrobial impacts. The disc diffusion test had been

Table 3  
Zone of inhibition observed against different fungal pathogens with different concentrations by disc diffusion method.

Pathogens	Zone of inhibition (mm)		
	TiO <sub>2</sub> NPs (µg/ml)		
	20	30	40
<i>A. niger</i>	21 ± 0.46	22 ± 0.49	27 ± 0.36
<i>A. flavus</i>	24 ± 0.33	30 ± 0.42	36 ± 0.46
<i>R. oryzae</i>	18 ± 0.35	27 ± 0.33	34 ± 0.31
<i>S. rolfisii</i>	24 ± 0.34	34 ± 0.31	42 ± 0.25

Results are expressed as mean ± SE.

used to evaluate the effectiveness of TiO<sub>2</sub> NPs against bacterial strains like *E. coli*, *S. aureus*, *P. aeruginosa*, *E. faecalis*, *K. pneumoniae* and *B. subtilis* and the diameter of the bacterial inhibition zone depends upon the solubility and infusibility of the titanium dioxide nanoparticles. Micro broth dilution assay was used to determine the MIC of TiO<sub>2</sub> nanoparticles against test bacterial strains. The lack of turbidity in cultural broth indicates the lowest concentration of TiO<sub>2</sub> nanoparticles. In antifungal action, utilizing disc diffusion assay against *A. niger*, *A. flavus*, *R. oryzae* and *S. rofsii*, the titanium dioxide nanoparticles were effectively inhibited all the test microbes as compared to control. Besides, the ability of the bacterial cell membrane plays a significant role in cell communication, which has closely related to apoptosis. The biological synthesis of TiO<sub>2</sub> nanoparticles could be a promising process for production of other metal oxide nanoparticles which could have natural, significant, drug and clinical applications.

### Declaration of Competing Interest

The authors declare that they have no known competing financial interests or personal relationships that could have appeared to influence the work reported in this paper.

### Acknowledgements

The authors acknowledge King Saud University, Riyadh, Saudi Arabia for funding this research through Researchers Supporting Project No. RSP 2022/11. The authors thank Sudan University of Science and Technology, Sudan for the support and encouragement.

### References

- Abdelhalim, M.A.K., Mady, M.M., Ghannam, M.M., 2012. Physical properties of different gold nanoparticles: ultraviolet-visible and fluorescence measurements. *J. Nanomed. Nanotechnol.* 3 (3), 178–194.
- Ahmad, R., Mohsin, M., Ahmad, T., Sardar, M., 2015. Alpha amylase assisted synthesis of TiO<sub>2</sub> nanoparticles: structural characterization and application as antibacterial agents. *J. Hazard. Mater.* 283, 171–177.
- Ahmad, N., Sharma, S., Alam, M.K., Singh, V.N., Shamsi, S.F., Mehta, B.R., Fatma, A., 2010. Rapid synthesis of silver nanoparticles using dried medicinal plant of basil. *Colloids Surf., B* 81 (1), 81–86.
- Ahmed, S., Ahmad, M., Swami, B.L., Ikram, S., 2016. A review on plants extract mediated synthesis of silver nanoparticles for antimicrobial applications: a green expertise. *J. Adv. Res.* 7 (1), 17–28.
- Aina, A.D., OluwafayokeOwolo, O., Aina, F.O., Majolagbe, O.N., OluKanni, O.D., Stephen, M.C., Aderiike, G., 2018. Biosynthesis of silver nanoparticles using almond plant leaf extract and their antibacterial activity. *Int. J. Eng. Sci.*, 19227.
- Akhtar, S., Ali, I., Tauseef, S., 2016. Synthesis, characterization and antibacterial activity of titanium dioxide (TiO<sub>2</sub>) nanoparticles. *FUUAST J. Biol.* 6 (2), 141–147.
- Akiba, N., Hayakawa, I., Keh, E.S., Watanabe, A., 2005. Antifungal effects of a tissue conditioner coating agent with TiO<sub>2</sub> photocatalyst. *Journal of medical and dental sciences* 52 (4), 223–227.
- Allahverdiyev, A.M., Abamor, E.S., Bagirova, M., Rafailovich, M., 2011. Antimicrobial effects of TiO<sub>2</sub> and Ag<sub>2</sub>O nanoparticles against drug-resistant bacteria and leishmania parasites. *Future Microbiol.* 6 (8), 933–940.
- Ambika, S., Sundrarajan, M., 2016. [EMIM] BF<sub>4</sub> ionic liquid-mediated synthesis of TiO<sub>2</sub> nanoparticles using Vitex negundo Linn extract and its antibacterial activity. *J. Mol. Liq.* 221, 986–992.
- Anitha, J., Miruthula, S., 2014. Traditional medicinal uses, phytochemical profile and pharmacological activities of *Luffa acutangula* Linn. *Int. J. Pharmacog.* 1 (3), 174–183.
- Anju, V.T., Paramanatham, P., Sruthil Lal, S.B., Sharan, A., Syed, A., Bahkali, N.A., Alsaedi, M.H., Kaviyarasu, K., Busi, S., 2019. Antimicrobial photodynamic activity of toluidine blue-carbon nanotube conjugate against *Pseudomonas aeruginosa* and *Staphylococcus aureus*—understanding the mechanism of action. *Photodiagn. Photodyn. Ther.* 27, 305–316.
- Brown, A.N., Smith, K., Samuels, T.A., Lu, J., Obare, S.O., Scott, M.E., 2012. Nanoparticles functionalized with ampicillin destroy multiple-antibiotic-resistant isolates of *Pseudomonas aeruginosa* and *Enterobacter aerogenes* and methicillin-resistant *Staphylococcus aureus*. *Appl. Environ. Microbiol.* 78 (8), 2768–2774.
- Buszewski, B., Railean-Plugaru, V., Pomastowski, P., Rafinska, K., Szultka-Mlynska, M., Golinska, P., Wypij, M., Laskowski, D., Dahm, H., 2018. Antimicrobial activity of biosilver nanoparticles produced by a novel *Streptacidiphilus durhamensis* strain. *J. Microbiol. Immunol. Infect.* 51 (1), 45–54.
- Chen, J., Zhang, H., Liu, P., Wang, Y., Liu, X., Li, G., An, T., Zhao, H., 2014. Vapor-phase hydrothermal synthesis of rutile TiO<sub>2</sub> nanostructured film with exposed pyramid-shaped (1 1 1) surface and superiorly photoelectrocatalytic performance. *J. Colloid Interface Sci.* 429, 53–61.
- Colthup, N.B., 1950. Spectra-structure correlations in the infra-red region. *JOSA* 40 (6), 397–400.
- Dadkhah, M., Salavati-Niasari, M., Mir, N., 2014. Synthesis and characterization of TiO<sub>2</sub> nanoparticles by using new shape controllers and its application in dye sensitized solar cells. *J. Ind. Eng. Chem.* 20 (6), 4039–4044.
- Dandge, V.S., Rothe, S.P., Pethe, A.S., 2010. Antimicrobial activity and pharmacognostic study of *Luffa acutangula* Roxb var amara on some deuteromycetes fungi. *Int. J. Sci. Innovat. Discov.* 2 (1), 191–196.
- Duan, H., Wang, D., Li, Y., 2015. Green chemistry for nanoparticle synthesis. *Chem. Soc. Rev.* 44 (16), 5778–5792.
- Fabrega, C., Andreu, T., Cabot, A., Morante, J.R., 2010. Location and catalytic role of iron species in TiO<sub>2</sub>: Fe photocatalysts: an EPR study. *J. Photochem. Photobiol., A* 211 (2–3), 170–175.
- Fang, F., Kennedy, J., Manikandan, E., Futter, J., Markwitz, A., 2012. Morphology and characterization of TiO<sub>2</sub> nanoparticles synthesized by arc discharge. *Chem. Phys. Lett.* 521, 86–90.
- French, R.A., Jacobson, A.R., Kim, B., Isley, S.L., Penn, R.L., Baveye, P.C., 2009. Influence of ionic strength, pH, and cation valence on aggregation kinetics of titanium dioxide nanoparticles. *Environ. Sci. Technol.* 43 (5), 1354–1359.
- Fu, D.G., Zhang, Y., Wang, X., Liu, J.Z., Lu, Z.H., 2001. Surface second order optical nonlinearity of titanium dioxide sized in nanometer range. *Chem. Lett.* 30 (4), 328–329.
- Geetha, N., Sivarajani, S., Ayeshamariam, A., Siva Bharathy, M., Nivetha, S., Kaviyarasu, K., Jayachandran, M., 2018. High performance photo-catalyst based on nanosized ZnO-TiO<sub>2</sub> nanoplatelets for removal of RhB under visible light irradiation. *J. Adv. Microsc. Res.* 13 (1), 12–19.
- Geethalakshmi, R., Sarada, D.V.L., 2010. Synthesis of plant-mediated silver nanoparticles using *Trianthema decandra* extract and evaluation of their antimicrobial activities. *Int. J. Eng. Sci. Technol.* 2 (5), 970–975.
- Gelis, C., Girard, S., Mavon, A., Delverdiere, M., Pailous, N., Vicendo, P., 2003. Assessment of the skin photoprotective capacities of an organo-mineral broad-spectrum sunblock on two ex vivo skin models. *Photodermatol. Photoimmunol. Photomed.* 19 (5), 242–253.
- Gelover, S., Gomez, L.A., Reyes, K., Leal, M.T., 2006. A practical demonstration of water disinfection using TiO<sub>2</sub> films and sunlight. *Water Res.* 40 (17), 3274–3280.
- George, A., Magimai Antoni Raj, D., Venci, X., Dhayal Raj, A., Albert Irudayaraj, A., Josephine, R.L., John Sundaram, S., Al-Mohameed, A.A., Al Farraj, D.A., Chen, T.-W., Kaviyarasu, K., 2022. Photocatalytic effect of CuO nanoparticles flower-like 3D nanostructures under visible light irradiation with the degradation of methylene blue (MB) dye for environmental application. *Environ. Res.* 203.
- Gerhardt, L.C., Jell, G.M.R., Boccaccini, A.R., 2007. Titanium dioxide (TiO<sub>2</sub>) nanoparticles filled poly (D, L lactic acid)(PDLA) matrix composites for bone tissue engineering. *J. Mater. Sci. - Mater. Med.* 18 (7), 1287–1298.
- Gong, P., Li, H., He, X., Wang, K., Hu, J., Tan, W., Zhang, S., Yang, X., 2007. Preparation and antibacterial activity of Fe<sub>3</sub>O<sub>4</sub>/Ag nanoparticles. *Nanotechnology* 18, (28) 285604.
- Habimana, O., Steenkeste, K., Fontaine-Aupart, M.P., Bellon-Fontaine, M.N., Kulakauskas, S., Briandet, R., 2011. Diffusion of nanoparticles in biofilms is altered by bacterial cell wall hydrophobicity. *Appl. Environ. Microbiol.* 77 (1), 367–368.
- Hoffmann, M.R., Martin, S.T., Choi, W., Bahnemann, D.W., 1995. Environmental applications of semiconductor photocatalysis. *Chem. Rev.* 95 (1), 69–96.
- Holt, K.B., Bard, A.J., 2005. Interaction of silver (I) ions with the respiratory chain of *Escherichia coli*: an electrochemical and scanning electrochemical microscopy study of the antimicrobial mechanism of micromolar Ag<sup>+</sup>. *Biochemistry* 44 (39), 13214–13223.
- Hu, C.M.J., Aryal, S., Zhang, L., 2010. Nanoparticle-assisted combination therapies for effective cancer treatment. *Therapeutic Delivery* 1 (2), 323–334.
- Hunagund, S.M., Desai, V.R., Kadadevarmath, J.S., Barretto, D.A., Vootla, S., Sidarai, A. H., 2016. Biogenic and chemogenic synthesis of TiO<sub>2</sub> NPs via hydrothermal route and their antibacterial activities. *RSC Adv.* 6 (99), 97438–97444.
- James, M.R., Cohen, J.B., 1980. The measurement of residual stresses by X-ray diffraction techniques. In: *Treatise on Materials Science & Technology*, pp. 1–62.
- Jayakumar, G., Irudayaraj, A.A., Raj, A.D., Sundaram, S.J., Kaviyarasu, K., 2022. Electrical and magnetic properties of Ni doped CeO<sub>2</sub> nanostructured for optoelectronic applications. *J. Phys. Chem. Solids* 160, 110369.
- Jayaseelan, C., Ramkumar, R., Rahuman, A.A., Perumal, P., 2013. Green synthesis of gold nanoparticles using seed aqueous extract of *Abelmoschus esculentus* and its antifungal activity. *Ind. Crops Prod.* 45, 423–429.
- Jayaseelan, C., Rahuman, A.A., Roopan, S.M., Kirthi, A.V., Venkatesan, J., Kim, S.K., Iyappan, M., Siva, C., 2013. Biological approach to synthesize TiO<sub>2</sub> nanoparticles using *Aeromonas hydrophila* and its antibacterial activity. *Spectrochim. Acta Part A Mol. Biomol. Spectrosc.* 107, 82–89.
- Kasinathan, K., Kennedy, J., Elayaperumal, M., Henini, M., Malik, M., 2016. Photodegradation of organic pollutants RhB dye using UV simulated sunlight on ceria based TiO<sub>2</sub> nanomaterials for antibacterial applications. *Sci. Rep.* 6 (1), 1–12.
- Kaviya, M., Ramakrishnan, P., Mohamed, S.B., Ramakrishnan, R., Gimbin, J., Veerabadran, K.M., Kuppusamy, M.R., Kaviyarasu, K., Sridhar, T.M., 2021.

- Synthesis and characterization of nano-hydroxyapatite/graphene oxide composite materials for medical implant coating applications. *Mater. Today Proc.* 36, 204–207.
- Kayalvizhi, K., Alhaji, N.M.I., Saravanakumar, D., Beer Mohamed, S., Kaviyarasu, K., Ayeshamariam, A., Al-Mohaimed, A.M., AbdelGawwad, M.R., Elshikh, M.S., 2022. Adsorption of copper and nickel by using sawdust chitosan nanocomposite beads—A kinetic and thermodynamic study. *Environ. Res.* 203, 111814.
- Kirthi, A.V., Rahuman, A.A., Rajakumar, G., Marimuthu, S., Santhoshkumar, T., Jayaseelan, C., Elango, G., Zahir, A.A., Kamaraj, C., Bagavan, A., 2011. Biosynthesis of titanium dioxide nanoparticles using bacterium *Bacillus subtilis*. *Mater. Lett.* 65 (17–18), 2745–2747.
- Li, X., Robinson, S.M., Gupta, A., Saha, K., Jiang, Z., Moyano, D.F., Sahar, A., Riley, M.A., Rotello, V.M., 2014. Functional gold nanoparticles as potent antimicrobial agents against multi-drug-resistant bacteria. *ACS Nano* 8 (10), 10682–10686.
- Lonnen, J., Kilvington, S., Kehoe, S.C., Al-Touati, F., McGuigan, K.G., 2005. Solar and photocatalytic disinfection of protozoan, fungal and bacterial microbes in drinking water. *Water Res.* 39 (5), 877–883.
- Loo, Y.Y., Rukayadi, Y., Nor-Khaizura, M.A.R., Kuan, C.H., Chieng, B.W., Nishibuchi, M., Radu, S., 2018. In vitro antimicrobial activity of green synthesized silver nanoparticles against selected gram-negative foodborne pathogens. *Front. Microbiol.* 9, 1555.
- Magdalane, C.M., Kaviyarasu, K., Raja, A., Arularasu, M.V., Mola, G.T., Isaev, A.B., Maaza, M., 2018. Photocatalytic decomposition effect of erbium doped cerium oxide nanostructures driven by visible light irradiation: investigation of cytotoxicity, antibacterial growth inhibition using catalyst. *J. Photochem. Photobiol., B* 185, 275–282.
- Magdalane, C.M., Priyadharini, G.M.A., Kaviyarasu, K., Jothi, A.I., Simiyon, G.G., 2021. Synthesis and characterization of TiO<sub>2</sub> doped cobalt ferrite nanoparticles via microwave method: investigation of photocatalytic performance of congo red degradation dye. *Surf. Interfaces* 25, 101296.
- Mani, M., Pavithra, S., Mohanraj, K., Kumaresan, S., Alotaibi, S.S., Eraqi, M.M., Gandhi, A.D., Ranganathan Babujanathanam, M., Maaza, K.K., 2021. Studies on the spectrometric analysis of metallic silver nanoparticles (Ag NPs) using *Basella alba* leaf for the antibacterial activities. *Environ. Res.* 199, 111274.
- Mani, M., Harikrishnan, R., Purushothaman, P., Pavithra, S., Rajkumar, P., Kumaresan, S., Al, D.A., Farraj, M.S., Elshikh, B.B., Kaviyarasu, K., 2021. Systematic green synthesis of silver oxide nanoparticles for antimicrobial activity. *Environ. Res.* 202, 111627.
- Mani, M., Okla, M.K., Selvaraj, S., Ram Kumar, A., Kumaresan, S., Muthukumar, A., Kaviyarasu, K., El-Tayeb, M.A., Elbadawi, Y.B., Almaary, K.S., Almunqedi, B.M.A., Elshikh, M.S., 2021. A novel biogenic *Allium cepa* leaf mediated silver nanoparticles for antimicrobial, antioxidant, and anticancer effects on MCF-7 cell line. *Environ. Res.* 198, 111199.
- Manjula, N., Selvan, G., Hameedha Bevi, A., Kaviyarasu, K., Ayeshamariam, A., Puthavelan, N., Jayachandran, M., 2018. Feasibility studies on avocado as reducing agent in TiO<sub>2</sub> doped with Ag<sub>2</sub>O and Cu<sub>2</sub>O nanoparticles for biological applications. *J. Bionanosci.* 12 (5), 652–659.
- Nalini, T., Basha, S.K., Sadiq, A.M.M., Kumari, V.S., Kaviyarasu, K., 2019. Development and characterization of alginate/chitosan nanoparticulate system for hydrophobic drug encapsulation. *J. Drug Delivery Sci. Technol.* 52, 65–72.
- Nithiyavathi, R., John Sundaram, S., Theophil Anand, G., Raj Kumar, D., Dhayal Raj, A., Al, D.A., Farraj, R.M., Aljowaie, M.R., AbdelGawwad, Y., Samson, K.K., 2021. Gum mediated synthesis and characterization of CuO nanoparticles towards infectious disease-causing antimicrobial resistance microbial pathogens. *J. Infect. Public Health* 14 (12), 1893–1902.
- Ocoy, I., Paret, M.L., Ocoy, M.A., Kunwar, S., Chen, T., You, M., Tan, W., 2013. Nanotechnology in plant disease management: DNA-directed silver nanoparticles on graphene oxide as an antibacterial against *Xanthomonas perforans*. *ACS Nano* 7 (10), 8972–8980.
- Orudzhev, F., Ramazanov, S., Sobola, D., Isaev, A., Wang, C., Magomedova, A., Kadiev, M., Kaviyarasu, K., 2020. Atomic layer deposition of mixed-layered Aurivillius phase on TiO<sub>2</sub> nanotubes: synthesis, characterization and photoelectrocatalytic properties. *Nanomaterials* 10 (11), 2183.
- Orudzhev, F.F., Ramazanov, M., Isaev, A.B., Alikhanov, N.M.R., Sobola, D., Yu Presniakov, M., Kaviyarasu, K., 2021. Self-organization of layered perovskites on TiO<sub>2</sub> nanotubes surface by atomic layer deposition. *Mater. Today Proc.* 36, 364–367.
- Panimalar, S., Logambal, S., Thambidurai, R., Imozhi, C., Uthrakumar, R., Muthukumar, A., Rasheed, R.A., Gatasheh, M.K., Raja, A., Kennedy, J., Kaviyarasu, K., 2022. Effect of Ag doped MnO<sub>2</sub> nanostructures suitable for wastewater treatment and other environmental pollutant applications. *Environ. Res.* 205, 112560.
- Paramantham, P., Antony, A.P., Sruthil Lal, S.B., Sharan, A., Syed, A., Ahmed, M., Alarfaj, A.A., Siddhardha Busi, M., Maaza, K.K., 2018. Antimicrobial photodynamic inactivation of fungal biofilm using amino functionalized mesoporous silica-rose bengal nanoconjugate against *Candida albicans*. *Sci. African* 1, e00007.
- Parasuraman, P., Antony, A.P., Sharan, A., Siddhardha, B., Kasinathan, K., Bahkali, N. A., Dawoud, T.M.S., Syed, A., 2019. Antimicrobial photodynamic activity of toluidine blue encapsulated in mesoporous silica nanoparticles against *Pseudomonas aeruginosa* and *Staphylococcus aureus*. *Biofouling* 35 (1), 89–103.
- P. Parasuraman, V.T. Anju, S.B. Sruthil Lal, Alok Sharan, Siddhardha Busi, K. Kaviyarasu, Mohammed Arshad, Turki M.S. Dawoud, Asad Syed, Synthesis and antimicrobial photodynamic effect of methylene blue conjugated carbon nanotubes on *E. coli* and *S. aureus*, *Photochem. Photobiol. Sci.* 18 (2), 563–576, 2019.
- Philipp, D., 2010. Rapid green synthesis of spherical gold nanoparticles using *Mangifera indica* leaf. *Spectrochim. Acta Part A Mol. Biomol. Spectrosc.* 77 (4), 807–810.
- Prakash, T., Navaneethan, M., Archana, J., Ponnusamy, S., Muthamizhchelvan, C., Hayakawa, Y., 2012. Synthesis of TiO<sub>2</sub> nanoparticles with mesoporous spherical morphology by a wet chemical method. *Mater. Lett.* 82, 208–210.
- Pu, X., Zhang, D., Gao, Y., Shao, X., Ding, G., Li, S., Zhao, S., 2013. One-pot microwave-assisted combustion synthesis of graphene oxide–TiO<sub>2</sub> hybrids for photodegradation of methyl orange. *J. Alloy. Compd.* 551, 382–388.
- Radhakrishnan, R., Lakshmi, D., Ali Khan, F.L., Ramalingam, G., Kaviyarasu, K., 2020. Bio-synthesis of iron oxide nanoparticles using neem leaf cake extract and its influence in the agronomical traits of vigna mungo plant. *Asian J. Nanosci. Mater.* 3 (1), 38–46.
- Rajakumar, G., Rahuman, A.A., Priyamvada, B., Khanna, V.G., Kumar, D.K., Sujin, P.J., 2011. Eclipta prostrata leaf aqueous extract mediated for the synthesis of titanium dioxide nanoparticles and its larvicidal activity against malaria vector. In: 2011 IEEE Nanotechnology Materials and Devices Conference. IEEE, pp. 563–566.
- Rajakumar, G., Rahuman, A.A., Priyamvada, B., Khanna, V.G., Kumar, D.K., Sujin, P.J., 2012. Eclipta prostrata leaf aqueous extract mediated synthesis of titanium dioxide nanoparticles. *Mater. Lett.* 68, 115–117.
- Rajeswari, R., Venugopal, D., Dhayal Raj, A., Arumugam, J., John Sundaram, S., Kaviyarasu, K., 2021. Effect of doping concentration for the properties of Fe doped TiO<sub>2</sub> thin films applications. *Mater. Today Proc.* 36, 468–474.
- Rajkumari, J., Maria Magdalane, C., Siddhardha, B., Madhavan, J., Ramalingam, G., Al-Dhabi, N.A., Arasu, M.V., Ghilan, A.K.M., Durairam, V., Kaviyarasu, K., 2019. Synthesis of titanium oxide nanoparticles using *Aloe barbadensis* mill and evaluation of its antibiofilm potential against *Pseudomonas aeruginosa* PAO1. *J. Photochem. Photobiol., B* 201, 111667.
- Ramesh, R., Yamini, V., Sundaram, S.J., Khan, F.L.A., Kaviyarasu, K., 2021. Investigation of structural and optical properties of NiO nanoparticles mediated by *Plectranthus amboinicus* leaf extract. *Mater. Today Proc.* 36, 268–272.
- Ramesh, R., Catherine, G., Sundaram, S.J., Khan, F.L.A., Kaviyarasu, K., 2021. Synthesis of Mn<sub>2</sub>O<sub>3</sub> nano complex using aqueous extract of *Helianthus annuus* seed cake and its effect on biological growth of *Vigna radiata*. *Mater. Today Proc.* 36, 184–191.
- Ramesh, R., Vidhya, V., Liakath, F., Khan, A., Muhammed Alnasrawi, A., Alkahtani, J., Elshikh, M.S., Kaviyarasu, K., 2022. Shockwave treated seed germination and physiological growth of *Vigna mungo* L in red soil environment. *Physiol. Mol. Plant Pathol.* 117, 101747.
- Rathnakumar, S.S., Noluthando, K., Kulandaiswamy, A.J., Rayappan, J.B., Kasinathan, K., Kennedy, J., Maaza, M., 2019. Stalling behaviour of chloride ions: a non-enzymatic electrochemical detection of  $\alpha$ -Endosulfan using CuO interface. *Sens. Actuators, B* 293, 100–106.
- Renuka, R., Renuka Devi, K., Sivakami, M., Thilagavathi, T., Uthrakumar, R., Kaviyarasu, K., 2020. Biosynthesis of silver nanoparticles using *Phyllanthus emblica* fruit extract for antimicrobial application, Biocatalysis and Agricultural. *Biotechnology* 24, 101567.
- Roopan, S.M., Bharathi, A., Prabhakaran, A., Rahuman, A.A., Velayutham, K., Rajakumar, G., Padmaja, R.D., Lekshmi, M., Madhumitha, G., 2012. Efficient phyto-synthesis and structural characterization of rutile TiO<sub>2</sub> nanoparticles using *Annona squamosa* peel extract. *Spectrochim. Acta Part A Mol. Biomol. Spectrosc.* 98, 86–90.
- Salunke, R.B., Patil, S.V., Patil, C.D., Salunke, B.K., 2011. Larvicidal potential of silver nanoparticles synthesized using fungus *Cochliobolus lunatus* against *Aedes aegypti* (Linnaeus, 1762) and *Anopheles stephensi* Liston (Diptera; Culicidae). *Parasitol. Res.* 109 (3), 823–831.
- Sathishkumar, M., Sneha, K., Won, S.W., Cho, C.W., Kim, S., Yun, Y.S., 2009. Cinnamon zeylanicum bark extract and powder mediated green synthesis of nano-crystalline silver particles and its bactericidal activity. *Colloids Surf., B* 73 (2), 332–338.
- Singh, M., Lee, K.E., Vinayagam, R., Kang, S.G., 2021. Antioxidant and antibacterial profiling of pomegranate-pericarp extract functionalized-zinc oxide nanocomposite. *Biotechnol. Bioprocess Eng.* 26 (5), 728–737.
- Singh, R., Lillard Jr, J.W., 2009. Nanoparticle-based targeted drug delivery. *Exp. Mol. Pathol.* 86 (3), 215–223.
- Srinivasan, S., Ramachandran, V., Murali, R., Vinothkumar, V., Raajasubramanian, D., Kanagalakshmi, A., 2020. Biogenic metal nanoparticles and their antimicrobial properties. In: *Nanotechnological Approaches in Food Microbiology*. CRC Press, pp. 403–413.
- Sundararajan, M., Bama, K., Bhavani, M., Jegatheeswaran, S., Ambika, S., Sangili, A., Nithya, P., Sumathi, R., 2017. Obtaining titanium dioxide nanoparticles with spherical shape and antimicrobial properties using *M. citrifolia* leaves extract by hydrothermal method. *J. Photochem. Photobiol., B* 171, 117–124.
- Trouiller, B., Reliene, R., Westbrook, A., Solaimani, P., Schiestl, R.H., 2009. Titanium dioxide nanoparticles induce DNA damage and genetic instability in vivo in mice. *Cancer Res.* 69 (22), 8784–8789.
- Vanajothi, R., Sudha, A., Manikandan, R., Rameshthangam, P., Srinivasan, P., 2012. Luffa acutangula and Lippia nodiflora leaf extract induces growth inhibitory effect through induction of apoptosis on human lung cancer cell line. *Biomed. Prevent. Nutr.* 2 (4), 287–293.

- Vazquez-Munoz, R., Avalos-Borja, M., Castro-Longoria, E., 2014. Ultrastructural analysis of *Candida albicans* when exposed to silver nanoparticles. *PLoS ONE* 9, (10) e108876.
- Velayutham, K., Rahuman, A.A., Rajakumar, G., Santhoshkumar, T., Marimuthu, S., Jayaseelan, C., Bagavan, A., Kirthi, A.V., Kamaraj, C., Zahir, A.A., Elango, G., 2012. Evaluation of *Catharanthus roseus* leaf extract-mediated biosynthesis of titanium dioxide nanoparticles against *Hippobosca maculata* and *Bovicola ovis*. *Parasitol. Res.* 111 (6), 2329–2337.
- Vijayakumar, S., Vinayagam, R., Anand, M.A.V., Venkatachalam, K., Saravanakumar, K., Wang, M.H., David, E., 2020. Green synthesis of gold nanoparticle using *Eclipta alba* and its antidiabetic activities through regulation of Bcl-2 expression in pancreatic cell line. *J. Drug Delivery Sci. Technol.* 58, 101786.
- Vinayagam, R., Santhoshkumar, M., Lee, K.E., David, E., Kang, S.G., 2021. Bioengineered gold nanoparticles using *Cynodon dactylon* extract and its cytotoxicity and antibacterial activities. *Bioprocess Biosyst. Eng.* 44 (6), 1253–1262.
- Vizhi, D.K., Supraja, N., Devipriya, A., Tollamadugu, N.V.K.V.P., Babujanathanam, R., 2016. Evaluation of antibacterial activity and cytotoxic effects of green AgNPs against Breast Cancer Cells (MCF 7). *Adv. Nano Res.* 4 (2), 129.
- Weir, A., Westerhoff, P., Fabricius, L., Hristovski, K., Von Goetz, N., 2012. Titanium dioxide nanoparticles in food and personal care products. *Environ. Sci. Technol.* 46 (4), 2242–2250.
- Wiley, J., 2001. *Sons* 1(11). New York; NY: Inc.
- Willner, I., Basnar, B., Willner, B., 2007. Nanoparticle–enzyme hybrid systems for nanobiotechnology. *FEBS J.* 274 (2), 302–309.
- Xiaoming, F., 2015. Synthesis and optical absorption properties of anatase TiO<sub>2</sub> nanoparticles via a hydrothermal hydrolysis method. *Rare Metal Mater. Eng.* 44 (5), 1067–1070.
- Zdyb, A., Krawczyk, S., 2014. Adsorption and electronic states of morin on TiO<sub>2</sub> nanoparticles. *Chem. Phys.* 443, 61–66.
- Zhang, H., Chen, G., 2009. Potent antibacterial activities of Ag/TiO<sub>2</sub> nanocomposite powders synthesized by a one-pot sol–gel method. *Environ. Sci. Technol.* 43 (8), 2905–2910.
- Zhao, W., Wang, H., Feng, X., Zhang, Y., Zhang, S., 2015. Control over the morphology of TiO<sub>2</sub> hierarchically structured microspheres in solvothermal synthesis. *Mater. Lett.* 158, 174–177.